

Optimized Dual Relay Deployment for LTE-Advanced Cellular Systems

Ahmed Hamdi

Egypt-Japan University of
Science and Technology (E-JUST)
Borg El-Arab, Alexandria, Egypt
a.hamdi@ieee.org

Mostafa El-Khamy^{*,‡}

* Egypt-Japan University of
Science and Technology (E-JUST)
‡ Faculty of Engineering, Alexandria University
m_elkhamy@ieee.org

Mohamed El-Sharkawy

Egypt-Japan University of
Science and Technology (E-JUST)
Borg El-Arab, Alexandria, Egypt
melshark@iupui.edu

Abstract—LTE-Advanced adopts relay deployment to support higher data rates and better coverage, especially at the cell edges which suffer from inter-cell interference. The solution of relaying is attractive because of its low cost and easy deployment. In this paper, we show that deploying just two relays per sector can significantly improve system capacity and coverage. We optimize the geometric deployment of relays that maximizes the spectral efficiency of the worst users or minimize outage. We consider the effects of different backhauling techniques such as wirelessly connected relays or wired radio remote heads. We also investigate the effect of different downlink frame structures and their impact on the system capacity or outage. The paper shows that the proper choice of the geometric deployment, frame structure and backhauling technique of the relays can improve the performance of LTE-Advanced.

Index Terms—Relay, LTE-Advanced, multihop, routing, capacity analysis, coverage extension.

I. INTRODUCTION

Relay Nodes (RNs) are adopted by 3GPP and are supported by the LTE-Advanced standard. RNs are deployed in cellular networks as they have the potential to enable next generation cellular systems meet the increasing demands for higher data rates, higher spectral efficiency and extended coverage [1]. Relay deployment also has the advantage of being a flexible, low cost solution as they can be connected wirelessly to the donor evolved-Node B (eNB). Deploying relays can alleviate the problem of cell-edge users (UEs) who suffer from low Signal-to-Interference-plus-Noise-Ratio (SINR) due to inter-cell interference.

There are several classifications of RNs [2], [3]. RNs can be classified into *amplify-and-forward* (AF) or *decode-and-forward* (DF) relays. The AF RN simply amplifies the received signal then forwards it. AF RNs cause negligible delays. However, AF RNs also amplify the noise, which can degrade the performance. DF RNs can perform some decoding protocols, so the noise is not propagated through data forwarding. The delay in DF RNs is large compared to AF RNs. Relay nodes can also be classified according to their mode of operation. In the *full-duplex* mode, the RN transmits and receives data simultaneously at the same time. On the other hand, in the *half-duplex* mode, the RN does not transmit when it is supposed to receive data. The later type reduces the interference problem when the backhaul link and access link; i.e., the link between

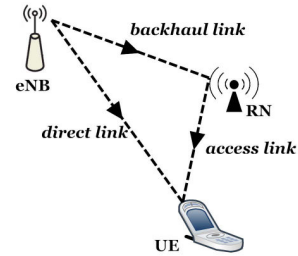


Fig. 1: Two-hop communication link

the RN and the UE, share the same carrier frequencies. In this paper, we use the half-duplex DF RNs as it is the most promising type.

Previous work in the literature that discuss the impact of deploying RNs on the cellular network performance do not consider the importance of the geometric deployment of RNs. In some work, it assumed that the RNs are deployed at a certain radius around the eNB with equal angle spacings [4], [5], [6]. Other work used the RN positions that were optimized for the IEEE 802.16m system [7].

In this paper, we propose a different RN deployment, for the case of two relays per sector, and show the impact of the geometric layout of the RNs on the system capacity and coverage. Our evaluation methodology takes into account the effect of the different downlink frame structures on the system performance. It also takes into account the effect of the capacity of the eNB-RN backhaul.

The rest of this paper is organized as follows. Section II presents the system model and frame structure. In section III, an analysis of the multihop relaying and relay routing algorithm is discussed. Our evaluation methodology is presented in section IV. In section V, our numerical simulation results are discussed. Section VI concludes the paper.

II. SYSTEM MODEL

In this paper, we assume that any UE can be served either by the eNB directly or by the RN via a two-hop link as shown in Fig. 1. We consider the ordinary hexagonal cellular layout with N_{eNB} sites, each with three sectors and each sector has two RNs as depicted in Fig. 2a. The frequency reuse factor is assumed to be 1; i.e., all sectors use the same frequency band. Fig. 2b shows our proposed positioning of the RNs with

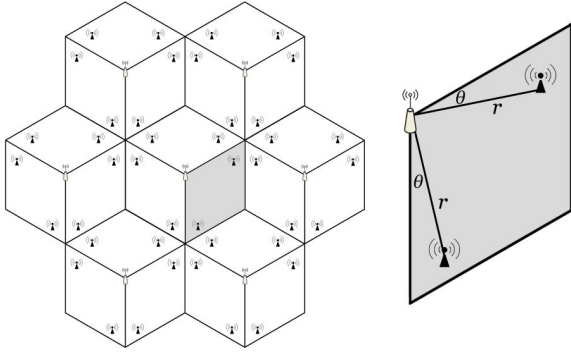


Fig. 2: RNs Deployment in a Cellular Network: (a) 7-Cell Layout and (b) RN Deployment per Sector

respect to the eNB. Each RN is positioned at the location (r, θ) where r is the distance between the RN and the eNB and θ is the angle between the eNB-RN direction and the closest sector edge. As shown below, we will optimize this deployment strategy to reduce the network coverage gaps and improve spectral efficiency.

With the LTE conventional frame structure, both eNBs and RNs will transmit simultaneously and thus interfere with each other. A relay node downlink frame structure is shown in Fig. 3, where the RN first receives the packets from the eNB in the backhaul subframe, and after decoding it, the RN re-encodes and retransmits the packets to the UE in the access subframe. This pair of downlink subframes is repeated periodically [8]. Different resource blocks are assigned for UEs with direct links and UEs with two-hop links.

III. SYSTEM ANALYSIS

In this section, we provide an SINR analysis and a capacity analysis of the cellular system in the presence of relays, and show how it is used in determining the relay routing algorithm.

A. SINR Analysis

When calculating the total interference I_{tot} for the conventional LTE frame structure ($\phi = 1$), we assume multiuser scheduling is done such that relays in the same sector do not interfere with their eNB sector. When adopting the RN downlink frame structure ($\phi = 0$), RNs and eNBs do not interfere with each other. It is assumed that the RNs of the same sector do not interfere with each other due to scheduling.

$$\phi = \begin{cases} 0 & \text{RN Downlink frame structure is used.} \\ 1 & \text{LTE conventional frame structure is used.} \end{cases} \quad (1)$$

The SINR of the direct link (Fig. 1) to UE u at coordinates (x, y) in sector s of eNB b is calculated as

$$SINR_u^{b,s}(x, y) = \frac{P_s^S h_u^{b,s}(x, y)}{I_{tot} + \sigma^2}, \quad (2)$$

$$I_{tot} = \sum_{i=1}^{N_{eNB}} \sum_{j=1}^{N_s} P_j^S h_u^{i,j}(x, y) - P_s^S h_u^{b,s}(x, y) + \phi \left(\sum_{i=1}^{N_{eNB}} \sum_{j=1}^{N_s} \sum_{k=1}^{N_r} P_k^R h_u^{i,j,k}(x, y) - \sum_{k=1}^{N_r} P_k^R h_u^{b,s,k}(x, y) \right),$$

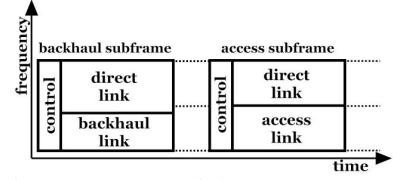


Fig. 3: RN Downlink Frame Structure

where $s = 1, \dots, N_s$, $b = 1, \dots, N_{eNB}$ and $r = 1, \dots, N_r$. N_{eNB} is number of eNBs, N_s is the number of sectors per eNB and N_r is the number of RNS per sector. P_s^S is the power transmitted from the s th sector and P_r^R is power transmitted from the r th RN. $h_u^{b,s,r}(x, y)$ and $h_u^{b,s}(x, y)$ are the total pathloss to UE u at coordinates (x, y) from the r th RN in the s th sector of the b th eNB and from the s th sector of the b th eNB, respectively. The pathloss includes all the transmitting and receiving antenna gains and the macroscopic pathloss. The thermal noise level at the receiver is σ^2 .

With few modifications to (2) and denoting the total pathloss from the s th sector of the b th eNB to RN r , the r th RN at coordinates (x, y) in the same sector, by $h_r^{b,s}(x, y)$, the SINR of the backhaul link to RN r is given by

$$SINR_r^{b,s}(x, y) = \frac{P_s^S h_r^{b,s}(x, y)}{I_{tot} + \sigma^2}, \quad (3)$$

$$I_{tot} = \sum_{i=1}^{N_{eNB}} \sum_{j=1}^{N_s} P_j^S h_r^{i,j}(x, y) - P_s^S h_r^{b,s}(x, y) + \phi \left(\sum_{i=1}^{N_{eNB}} \sum_{j=1}^{N_s} \sum_{k=1}^{N_r} P_k^R h_r^{i,j,k}(x, y) - \sum_{k=1}^{N_r} P_k^R h_r^{b,s,k}(x, y) \right).$$

Similarly, the SINR of the access link to UE u at coordinates (x, y) in sector s of eNB b and served by RN r is

$$SINR_u^{b,s,r}(x, y) = \frac{P_r^R h_u^{b,s,r}(x, y)}{I_{tot} + \sigma^2}, \quad (4)$$

$$I_{tot} = \sum_{i=1}^{N_{eNB}} \sum_{j=1}^{N_s} \sum_{k=1}^{N_r} P_k^R h_u^{i,j,k}(x, y) - \sum_{k=1}^{N_r} P_k^R h_u^{b,s,k}(x, y) + \phi \left(\sum_{i=1}^{N_{eNB}} \sum_{j=1}^{N_s} P_j^S h_u^{i,j}(x, y) - P_s^S h_u^{b,s}(x, y) \right).$$

B. Capacity Analysis

The point-to-point spectral efficiency (η) of a single-hop link for a given SINR value is given by Shannon's formula,

$$\eta = B_{eff} \log_2 \left(1 + \frac{SINR}{SINR_{eff}} \right), \quad (5)$$

where the bandwidth efficiency (B_{eff}) and the SINR efficiency ($SINR_{eff}$) are scaling parameters to make Shannon's formula fit with the adaptive modulation and coding curves considered in the LTE standard. It is found that when 64-QAM is set to be the highest modulation scheme, setting B_{eff} and $SINR_{eff}$ to 0.88 and 1.25 respectively, (5) gives an excellent match to practical measurements [9].

For an N -hop link, let η_n be the point-to-point spectral efficiency of the n th hop calculated by (5), then the effective end-to-end spectral efficiency η_{eff} can be calculated by [10]

$$\eta_{eff} = \left(\sum_{n=1}^N \frac{1}{\eta_n} \right)^{-1}. \quad (6)$$

C. Relay Routing Algorithm

In this paper, we use the effective spectral efficiency as the route selection metric. This metric is chosen to consider the extra resources used by the RN in the multihop connection. For a UE u at coordinates (x, y) and a RN r , we denote $\eta_b^s(r)$, $\eta_a^r(u)$ and $\eta_d^s(u)$ to respectively be the spectral efficiencies of the backhaul link from sector s to RN r , access link from RN r to UE u and direct link from sector s to UE u . $\eta_b^s(r)$, $\eta_a^r(u)$ and $\eta_d^s(u)$ are calculated by substituting (2), (3) and (4), respectively, in (5). Using (6), the two-hop link effective spectral efficiency (η_{2h}) for UE u through RN r is given by

$$\eta_{2h}^{s,r}(u) = \left(\frac{1}{\eta_b^s(r)} + \frac{1}{\eta_a^r(u)} \right)^{-1}.$$

The best route for UE u at coordinates (x, y) , denoted by $\mathcal{R}(x, y)$, can be determined as

$$\mathcal{R}(x, y) = \arg \max_{s,r} \{ \eta_d^s(u), \eta_{2h}^{s,r}(u) \}. \quad (7)$$

Wired radio remote heads (RRH) connected to the eNB via optical fiber cables will have a very high backhaul link capacity. In this case, the effective spectral efficiency will be constrained by the access link spectral efficiency; i.e. for a RRH r , sector s and UE u at (x, y) ,

$$\eta_{2h}^{s,r}(u) \approx \eta_a^r(u),$$

and the best route can be determined by

$$\mathcal{R}(x, y) = \arg \max_{s,r} \{ \eta_d^s(u), \eta_a^r(u) \}. \quad (8)$$

IV. SYSTEM EVALUATION METHODOLOGY

Our evaluation methodology aims to quantify the extent that RNs increase capacity, improve fairness or extend coverage. The minimum ten percentile throughput (or capacity) is widely accepted as a fairness measure, as cells with higher 10 %-tile throughput tend to have higher fairness. Furthermore, increasing the capacity at locations in the cell with the least received SINR, increases the overall system capacity. The cell outage is defined as the percentage of locations in the cell with received SINR less than a pre-specified threshold. A UE in such a location can experience call drops or acquisition failure. Cell outage is used as the performance metric for coverage extension.

We performed system level simulation of the LTE-Advanced system, following [11] with necessary modifications to include relay nodes. The LTE-Advanced simulation parameters used are summarized in Table I. The pathloss from the eNB to a location at distance R from the eNB is dependent whether it is at line of sight (LOS) or non-LOS (NLOS). The likelihood of a location being at LOS or NLOS is determined by the LOS probability function, $Prob(LOS)$ [1].

TABLE I: Simulation Parameters

Parameter	Value
System Parameters	
Carrier Frequency	2 GHz
Bandwidth	10 MHz
Bandwidth Efficiency	0.88
SINR Efficiency	1.25
Thermal Noise	-174 dBm/Hz
Propagation Model	
Model	Urban
Inter-site Distance	500 m
Pathloss (PL)	
$PL = PL(LOS) \cdot Prop(LOS) + PL(NLOS) \cdot Prop(NLOS)$	
$PL(LOS) = PL_{LOS} + 10 \cdot n_{LOS} \log_{10}(R)$	
$PL(NLOS) = PL_{NLOS} + 10 \cdot n_{NLOS} \log_{10}(R)$	
$Prob(LOS) = 1 - Prob(NLOS)$	
Direct Link:	
$PL_{LOS} = 103.4$	
$n_{LOS} = 2.42$	
$Prob(LOS) = \min(\frac{0.018}{R}, 1)(1 - \exp(-\frac{R}{0.063})) + \exp(-\frac{R}{0.063})$	
$PL_{NLOS} = 131.1$	
$n_{NLOS} = 4.28$	
Backhaul Link:	
$PL_{LOS} = 100.7$	
$n_{LOS} = 2.35$	
$Prob(LOS) = \min(\frac{0.018}{R}, 1)(1 - \exp(-\frac{R}{0.072})) + \exp(-\frac{R}{0.072})$	
Access Link:	
$PL_{LOS} = 103.8$	
$n_{LOS} = 2.09$	
$Prob(LOS) = 0.5 - \min(5 \cdot \exp(-\frac{0.156}{R}), 0.5) + \min(5 \cdot \exp(-\frac{R}{0.03}), 0.5)$	
$PL_{NLOS} = 145.4$	
$n_{NLOS} = 3.75$	
eNB Parameters	
Number of eNBs	7
Sector per eNB	3
Tx Power	46 dBm
Sector Antenna Gain	15 dB
Antenna Pattern	$A(\phi) = -\min(12(\frac{\phi}{70^\circ})^2, 25)$
Minimum Coupling Loss	70 dB
RN Parameters	
RN per Sector	2 RNs
Tx Power	30 dBm
Antenna Gain	5 dB
Antenna Pattern	Omni-directional
Minimum Coupling Loss	45 dB
Rx Noise Figure (NF)	5 dB
UE Parameters	
Antenna Gain	0 dB
Rx Noise Figure (NF)	9 dB

V. OPTIMIZED RN DEPLOYMENT RESULTS

The location of RNs in the cell provides an interesting tradeoff. When the RN is located close to the eNB, the RN will have a good connection of high SINR with the eNB, but UEs at the cell edge will have bad connections with both the RN and the eNB. However, when the RN is close to the cell-edge, UEs at the cell-edge will have a good connection with the RN, but the RN will not have a good connection with the eNB, thus affecting the quality of the end-to-end connection.

Through extensive system level simulations of the LTE-Advanced system, we optimize the geometrical deployment of relay nodes to maximize the cell spectral efficiency or extend the cell coverage. We show the possible gains from deploying two RNs per sector as in Fig. 2a in different scenarios (frame structure, wired or wireless relays). The optimum location of

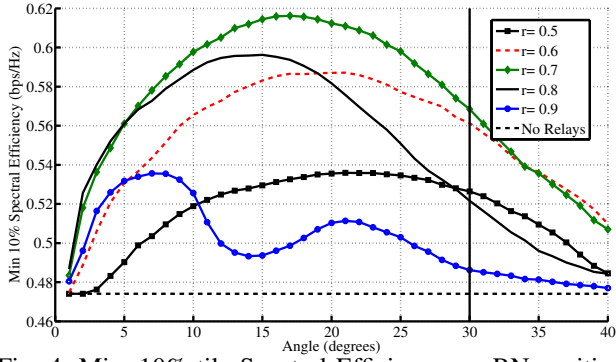


Fig. 4: Min. 10%-tile Spectral Efficiency vs. RN positions

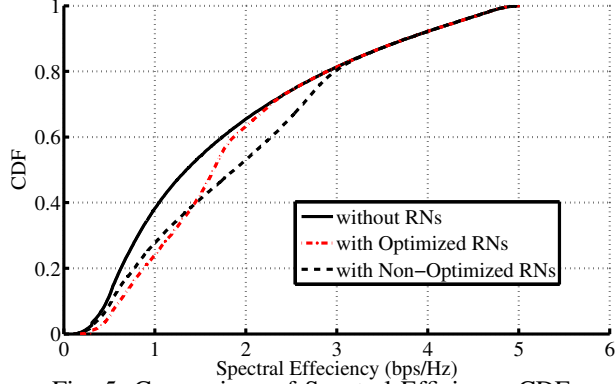


Fig. 5: Comparison of Spectral Efficiency CDFs

all RNs is given by (r_{opt}, θ_{opt}) , such that r_{opt} is represented as a fraction of the cell radius and θ_{opt} is measured from the sector edge as shown in Fig. 2b.

A. Spectral Efficiency-Optimized RN Deployment

In this subsection, we consider the case when the RNs deploy the RN downlink frame structure of Fig. 3 and have wireless backhaul links. The effective spectral efficiency at any location is that achieved by the best route determined by (7) for wireless backhauls or by (8) for wired backhauls. Fig. 4 shows the minimum 10%-tile effective spectral efficiency when the RNs are located at different radii and angles. We find that the optimum location of the two relays that maximizes the cell minimum 10%-tile spectral efficiency at 0.62 bps/Hz is

$$(r_{opt}, \theta_{opt}) = (0.7, 17^\circ). \quad (9)$$

This figure also shows the advantage of using our proposed RN deployment of Fig. 2 over the conventional equal angle spacing deployment, which is the special case of $\theta = 30^\circ$.

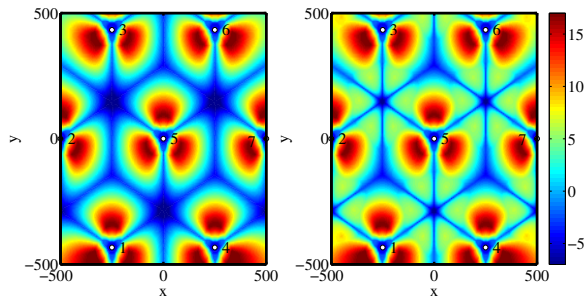


Fig. 6: SINR map: (a) without RNs and (b) with RNs

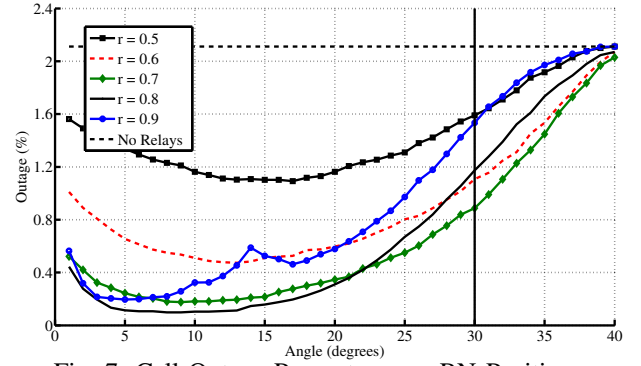


Fig. 7: Cell-Outlet Percentage vs. RN Positions

In Fig. 5, we show the cumulative distribution function (CDF) of the effective spectral efficiency for the optimized and non-optimized conventional equal angle spacing deployment cases. We observe that the RN deployments improve system fairness and throughput; it improves the spectral efficiency of the worst users (0.5 bps/Hz improvement at the 40 %-tile) without degrading the spectral efficiency at the good cell locations. Moreover, the optimized deployment improves the minimum 10%-tile spectral efficiency users compared to the non-optimized case. This is also illustrated by comparing the system SINR maps with the optimized RN deployment and without RNs in Fig. 6, which shows that our optimized deployment is successful in alleviating the cell-edge problem.

B. Coverage-Optimized RN Deployment

RN deployment offers another interesting tradeoff: deployment of RNs close to the cell-edge to cover eNB coverage-gaps will result in RNs of neighboring cells being very close to each other, and thus causing undesired interference to neighboring RNs and cell-edge UEs of neighboring cells. As in the previous subsection, the results here assume the RN downlink frame structure and wireless relays. However, here we optimize the location of the RNs that minimizes the cell outage, where the outage SINR threshold is set to -5 dB. The effective SINR is calculated by substituting the effective spectral efficiency of (7) in (5). The percentage of cell locations in SINR outage for different RN locations is shown in Fig. 7. The optimum position of RNs that minimizes cell outage is found to be

$$(r_{opt}, \theta_{opt}) = (0.8, 8.5^\circ). \quad (10)$$

C. Impact of Downlink Frame Structure

In this subsection, we investigate the advantage of using RN downlink frame structure of Fig. 3 over using the conventional LTE frame structure. For the case of wirelessly connected relays using the conventional LTE frame structure, the optimum position that maximizes the minimum 10%-tile spectral efficiency is

$$(r_{opt}, \theta_{opt}) = (0.8, 9^\circ). \quad (11)$$

Fig. 8 compares the CDF of the effective spectral efficiencies for the optimized deployments in both scenarios, RN downlink frame structure and conventional LTE frame structure. As

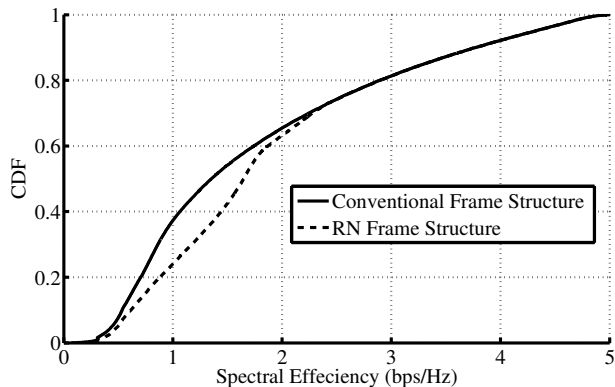


Fig. 8: Spectral Efficiency CDFs

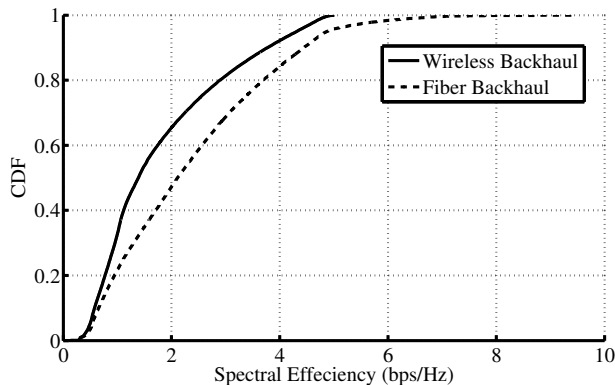


Fig. 9: Spectral Efficiency CDFs

expected, using the RN downlink frame structure resulted in more gain in effective spectral efficiency of the low SINR UEs.

The same position of (11) was also found to minimize the cell outage in case of conventional frame structure. However, the percentage of locations in outage is six times higher than that can be achieved with the RN downlink frame structure.

D. Impact of Backhaul Link Deployment

In this subsection, we discuss the effect of the backhaul link on the network performance. We compare the popular scenario of using RNs with wireless backhauls with the more expensive scenario of RNs with wired backhauls using fiber optics or microwave links. In case of wired RN backhauls and deploying the RN downlink frame structure, the effective spectral efficiencies is calculated by (8), and the optimum RN location that maximizes the minimum 10%-tile spectral efficiency is

$$(r_{opt}, \theta_{opt}) = (0.7, 18^\circ), \quad (12)$$

and the RN location which gives the minimum outage is

$$(r_{opt}, \theta_{opt}) = (0.8, 7.5^\circ). \quad (13)$$

Although the optimum locations are close to those of wireless backhauls, we note that wired backhauls increase the total cell capacity as shown by CDFs in Fig. 9. This is expected as wired backhauls guarantee a high SINR link from the eNB to the RN regardless of the location of the RN. Also, we observed that RN deployment with wired backhauls significantly reduce (by more than half) the cell locations in outage achieved with wireless backhauls.

VI. CONCLUSION

In this paper, we have studied different scenarios for deploying relay nodes (RNs) in LTE-Advanced cellular networks. We show that deploying only two relays per sector can significantly increase cell throughput, improve system fairness, and eliminate cellular coverage gaps caused by inter-cell interference. We optimize the geometric deployment of the relays and show that the optimized dual relay deployment achieves significant gains over conventional equal angle deployment. We quantify how different deployment scenarios can affect the performance of the LTE-Advanced system. We show that adopting a relay downlink frame structure improves system capacity and coverage through eliminating interference between RNs and eNBs. We also show that LTE-Advanced systems deploying more expensive relays with wired backhaul links have higher system capacity, fairness and coverage.

VII. ACKNOWLEDGMENT

This work is partially supported by the Missions Department of Egyptian Ministry of Higher Education (MoHE) and the 4G++ project of Egyptian National Telecom Regulatory Authority (NTRA).

REFERENCES

- [1] "Further Advancements of E-UTRA - Physical Layer Aspects (Release 9)," 3GPP, TR 36.814, Mar. 2010.
- [2] "Further details and considerations of different types of relays," 3GPP, TSG-RAN WG1 R1-083712, Sept. 2008.
- [3] K. Zheng, B. Fan, Z. Ma, G. Liu, X. Shen, and W. Wang, "Multihop cellular networks toward LTE-advanced," *Vehicular Technology Magazine, IEEE*, vol. 4, no. 3, pp. 40–47, 2009.
- [4] Z. Ma, K. Zheng, W. Wang, and Y. Liu, "Route Selection Strategies in Cellular Networks with Two-Hop Relaying," in *Wireless Communications, Networking and Mobile Computing, 2009. WiCom '09. 5th International Conference on*, Sept. 2009, pp. 1–4.
- [5] S. Peters, A. Panah, K. Truong, and R. Heath, "Relay architectures for 3GPP LTE-advanced," *EURASIP Journal on Wireless Communications and Networking*, vol. 2009, pp. 1–14, 2009.
- [6] M. Charafeddine, O. Oyman, and S. Sandhu, "System-level performance of cellular multihop relaying with multiuser scheduling," in *Information Sciences and Systems, 2007. CISS'07. 41st Annual Conference on*. IEEE, 2007, pp. 631–636.
- [7] M. Minelli, M. Coupechoux, J.-M. Kelif, M. Ma, and P. Godlewski, "Relays-enhanced LTE-Advanced networks performance studies," in *Sarnoff Symposium, 2011 34th IEEE*, May 2011, pp. 1–5.
- [8] "Evolved Universal Terrestrial Radio Access (E-UTRA); Physical Channels and Modulation (Release 8)," 3GPP, TSG-RAN 36.211, May 2009.
- [9] P. Mogensen, W. Na, I. Kovacs, F. Frederiksen, A. Pokhariyal, K. Pedersen, T. Kolding, K. Hugi, and M. Kuusela, "LTE capacity compared to the shannon bound," in *Vehicular Technology Conference, 2007. VTC2007-Spring. IEEE 65th*. IEEE, 2007, pp. 1234–1238.
- [10] O. Oyman and S. Sandhu, "A Shannon-theoretic perspective on fading multihop networks," in *Information Sciences and Systems, 2006 40th Annual Conference on*. IEEE, 2006, pp. 525–530.
- [11] J. C. Ikuno, M. Wrulich, and M. Rupp, "System level simulation of LTE networks," in *Proc. 2010 IEEE 71st Vehicular Technology Conference*, Taipei, Taiwan, May 2010.